# Cobalt Ion Mediated Self-Assembly of Genetically Engineered Bacteriophage for Biomimetic Co−Pt Hybrid Material

Soo-Kwan Lee,[†] Dong Soo Yun,[‡] and Angela M. Belcher*[,†,‡]

*Biological Engineering Division, Department of Materials Science and Engineering, Massachusetts Institute of Technology, 77 Massachusetts Avenue, Cambridge, Massachusetts 02139*

*Received September 19, 2005; Revised Manuscript Received November 4, 2005*

Biological scaffolds are used for the synthesis of inorganic materials due to their ability to self-assemble and nucleate crystal formation. We report the self-assembly of engineered M13 bacteriophage as a template for Co−Pt crystals. A M13 phage library with an octapeptide library on the major coat protein (pVIII) was used for selection of binders to cobalt ions. Fibrous structures with directionally ordered M13 phage were obtained by interaction with cobalt ions. Co−Pt alloys were synthesized on the fibrous scaffold, and their magnetic properties were characterized. The mineralization showed organized nanoparticles on fibrous bundles. This approach using the phage pVIII library allows for genetic selection that both induces assembly of the phage and directs mineralization of the selected inorganic material.

## Introduction

Precise recognition and self-assembly are required for the proper structure and function of a biological component such as actin filaments, microtubules, and chromatin. Due to their ability to interact with high specificity on the nanoscale level, biomaterials are potential building blocks for the nucleation and self-assembly of inorganic materials. Biological templates, such as DNA,[1] amphiphilic peptides,[2] and artificial proteins,[3] have been introduced for the "bottom up" biomimetic fabrication of supramolecular architectures. In nature, matrixes of biological macromolecules form mechanical frameworks in biomineralization systems, such as collagen (bone),[4,5] silicatein (silica sponges),[6,7] cellulose (plant silica), $\beta$-chitin (crab cuticle, mollusk shells),[8,9] and lustrin A (mollusk shells).[10] However, the use of biological macromolecules for biomineralization in vitro is more limited due to the ability to synthesis and purify the complex macromolecules required for the controlled synthesis of the material.

Peptides that have specificity for inorganic compounds have been selected using peptide libraries[11,12] and used successfully for the nucleation and growth control of the inorganic nanoparticles in aqueous solution at room temperature.[13,14] Filamentous bacteriophages (f1, fd, and M13) are excellent biological building blocks due to their controllable length and ability to display multiple peptides. The wild-type filamentous bacteriophage is approximately 930 nm in length and 6 nm in diameter. The phage surface consists of five capsid proteins (pIII, pVI, pVII, pVIII, and pIX). The pIII protein is expressed in five copies at the end of the phage and is commonly used to display foreign molecules, such as natural peptides, random peptides, proteins, and protein domains. The major coat protein, pVIII, is expressed in 2700 copies per phage and forms the cylindrical structure that surrounds the viral single stranded DNA (ssDNA). Type 8 phage display systems have been introduced, in which the pVIII proteins have been modified to display selected octapeptides. The peptides are displayed at distances approximately 2.7 nm from one another and have included antigenic epitopes (ConA), peptide that specifically bind to small molecules (dioxin), and those that confer chloroform resistance.[15] The homogeneous type 8 phage have defined lengths and could be used as genetically programmed biological scaffolds for inorganic materials.

**Scheme 1.** Schematic Diagram Illustrating Formation of Co−Pt Hybrid Material Using a Self-Assembled Phage Framework (Orange Dots = Cobalt Ions, Black Dots = Co−Pt)

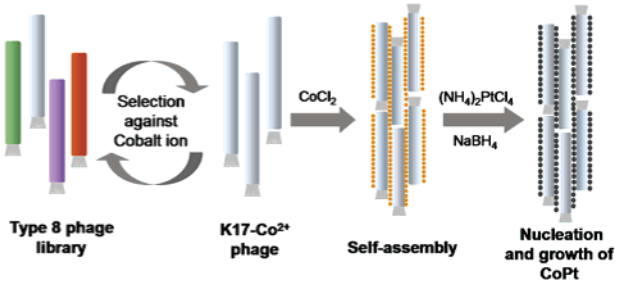


Nanophase Co−Pt alloys have been studied extensively in the past as a magnetic material, due to the high magnetocrystalline anisotropy, $\sim 5 \times 10^7$ ergs/cm$^3$ for the face-centered tetragonal (fct) phase. Here, we used the genetically engineered type 8 phage library to select phage that displayed peptides with affinity for the cobalt ion. The selected type 8 phage were then used to form the biological mechanical framework for a bioinorganic (Co−Pt) hybrid material by cobalt ion mediated self-assembly (Scheme 1).

## Experimental Section

**Materials.** All chemicals were obtained from Sigma Aldrich unless otherwise noted. M13KE phage vector, *Pst* I, *Bam*H I, and Klenow fragment (3′→ 5′ exo$^-$) were purchased from New England Biolabs (NEB). Oligonucleotides were from Integrated DNA Technologies. XL1-Blue Electroporation Competent Cells were obtained from Stratagene. Chelating Sepharose Fast Flow gel was purchased form Amersham Biosciences. 2−40% TBE polyacrylamide gel was from Invitrogen. dNTP was purchased form Promega. Tris buffered saline (TBS) solution (pH 7.5) was prepared in house from NaCl (Mallinckodt Chemicals) and Tris base (Roche).

**Type 8 Phage Library.** The M13KE phage vector was modified by making a cloning site for pVIII display as described previously.[15] A *Pst* I restriction site was made by mutating T to A at position 1372,

* To whom correspondence should be addressed. E-mail: belcher@mit.edu.
[†] Biological Engineering Division.
[‡] Department of Materials Science and Engineering.

10.1021/bm050691x CCC: $33.50 
Published on Web 11/24/2005

a *Bam*H I site was made by mutating C to G at positon 1381, and the *Pst* I site at position 6246 was deleted by mutating T to A at position 6250. The site-directed mutagenesis was done using overlap extension PCR. A dsDNA library was then prepared and cloned into the resulting modified phage vector, named M13SK, using *Pst* I and *Bam*H I. To obtain the dsDNA library, partial library duplexes were formed by annealing of extension primer (5′-GATGCTGTCTTTCGCTGCAG-3′) with oligonucleotides (3′-ACGACAGAAAGCGACGTC*nm*(*nnm*)$_6$*nn*-CCTAGGAACATC ATC-5′, where $n$ = A, T, C, or G and $m$ = A or C). The partial library duplexes were incubated with Klenow fragment (3′→ 5′ exo$^-$) (10 U/$\mu$L) and dNTP at 37 °C for 30 min. The Klenow fragment was inactivated by heating (75 °C for 20 min), and the mixture was digested with *Pst* I and *Bam*H I. The digested DNA was gel purified (2−40% TBE polyacrylamide gel), ligated into M13SK, and transfected to XL1-Blue Electroporation Competent Cells using a MicroPulser (Biorad). The library was titered according to manufacturer directions and sequenced (MIT Biopolymers Laboratory) before amplification. The estimated random population of the type 8 phage library was $10^7$∼$10^8$ pfu from the titering.

**Biopanning.** The selection of type 8 phage with affinity toward $Co^{2+}$ was performed by incubating the type 8 phage library (∼$10^{10}$ pfu) with $Co^{2+}$ immobilized on 200 $\mu$L of Chelating Sepharose Fast Flow gel in TBS buffer (pH 7.5) with 0.15% tween-20. The bound phage were washed 10 times with the incubation buffer and then eluted with 50 mM histidine. The fourth elution was amplified for the next round of biopanning. After the fourth round, the eluted phage was amplified, and the sequence was conformed.

**Synthesis of CoPt on Phage Templates.** The K17−$Co^{2+}$ phage ($1 \times 10^8$ pfu/$\mu$L) was incubated with 3.75 mM cobalt(II) chloride hexahydrate ($CoCl_2 \cdot 6H_2O$) in TBS buffer (pH 7.5) at room temperature for 30 min. The mixture was then incubated with ammonium tetrachloroplatinate ($(NH_4)_2PtCl_4$, 1.25 mM final concentration) at room temperature for 30 min before being reduced with sodium borohydride ($NaBH_4$, 1.25 mM final concentration).

**Characterization.** Polarized optical microscopy (Olympus) was used for optical microscopy and cross-polarized optical microscopy (CPOM) images. Transmission electron microscopy (TEM) and high-resolution TEM (HRTEM) images were obtained using JEOL 200CX and JEOL 2010 TEMs (JEOL), respectively, at an accelerating voltage of 200 kV. Energy dispersive spectroscopy (EDS) and chemical element mapping data were taken using an HB603 Scanning TEM (STEM) at 250 kV. Scanning electron microscopy (SEM) images were obtained using a JEOL 6320FV field-emission SEM at 1 kV after dialysis, freeze-drying, and gold sputter coating. Magnetic properties were characterized using a DC superconducting quantum interference device magnetometer (DC SQUID) (Quantum Design). The effective magnetic anisotropy energy density ($K_{eff}$) can be estimated by Neel's theory[16]

$$25k_BT_B = K_{eff}V \quad (1)$$

where $k_B$ is the Boltzmann constant and $V$ is an average volume of particles. The true magnetic moment at a particular temperature above $T_B$ was calculated by fitting the magnetization curve (Figure 4c) to the Langevin function[17,18]

$$M = M_s\left(\coth\left(\frac{\mu H}{k_BT}\right) - \frac{k_BT}{\mu H}\right) \quad (2)$$

where $\mu$ is the true magnetic moment of each nanoparticle, $M_s$ is the saturation magnetization, $T$ is the absolute temperature, and $H$ is the applied magnetic field.

## Results and Discussion

After four rounds of biopanning against $Co^{2+}$ using the type 8 phage library, a dominant $Co^{2+}$ binding phage displaying the octapeptide, EPGHDAVP, was selected. The peptide sequence contained a well-known metal binding motif, EXXH, which can be found within active sites of metalloproteins, an especially diverse class of diiron proteins. The active sites consist of a four-helix bundle coordinated by metal ions.[19,20]

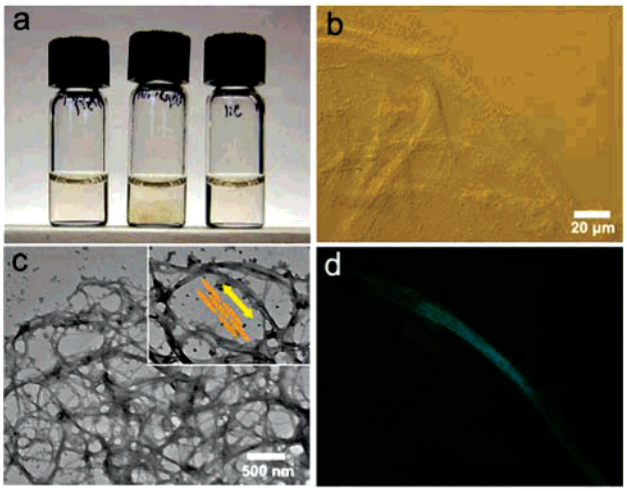


**Figure 1.** (a) Photograph of cobalt mediated fibrils in solution using wild-type (left), K17−$Co^{2+}$ (center), and no phage (right). (b) Optical microscopy image and (c) TEM image of the fibrils (from center sample). Inset: directional placement of phage particle along the bundle (d) Cross-POM image of (b).

The selected type 8 phage, named K17−$Co^{2+}$, was used for $Co^{2+}$ mediated self-assembly of phage. $CoCl_2$ (3.75 mM in TBS pH 7.5) was incubated with $1 \times 10^8$ pfu/$\mu$L of K17−$C^{2+}$ or wild-type (M13KE) phage. Phage bundles were observed in the sample containing the K17−$Co^{2+}$ phage after 30 min (Figure 1a, center) but were absent in the samples containing the wild-type phage (left) and no phage (right). CPOM revealed birefringence in the phage bundle (Figure 1d) indicating the bundle formation with directional order. A transmission electron micrograph of the bundles positively stained with uranyl acetate (1%) showed a spongelike texture (Figure 1c), in which the direction of the bundle is parallel to the long axis of the phage particles. The directional order of the rodlike molecules has been shown to be dependent on their concentration and the force applied.[21] In these experiments, the addition of cobalt ions stimulated the formation of bundles with directional ordering at phage concentrations much lower (∼$10^8$ pfu/$\mu$L) than that required for liquid crystalline (LC) formation (∼$10^{12}$ pfu/$\mu$L).[22] The directional ordering could be due to increased local concentration of phage and induced interactions between phage particles.

Co−Pt nanoparticles were then synthesized on the phage bundles by adding $(NH_4)_2PtCl_4$ to the solutions and reducing them with $NaBH_4$. Mineralization of Co−Pt was observed on the darkened fibrous networks of K17−$Co^{2+}$ phage (Figure 2a, center) but not in the solutions containing wild-type phage (left) and no phage (right). The wild-type phage did not form the fibrous structure in the presence of cobalt ions, and an aggregate of black precipitation was observed in the vial. The presence of Co and Pt was confirmed by using EDS. Structures with the composition $Co_{0.35}Pt_{0.65}$ were observed with K17−$Co^{2+}$ phage, whereas structures with composition $Co_{0.25}Pt_{0.75}$ were observed with wild-type or no phage. The difference can be due to different local concentration of cobalt near surface of the phage particles. The hybrid $Co_{0.35}Pt_{0.65}$ phage material was dialyzed and freeze-dried, and its microscale texture was examined by SEM (Figure 2b). Crystal growth on the oriented phage fibrils was characterized by using TEM (Figure 2c,d). The stripe patterns observed on the bundles are ∼6 nm in width, close to the diameter of a phage particle. The selected area electron

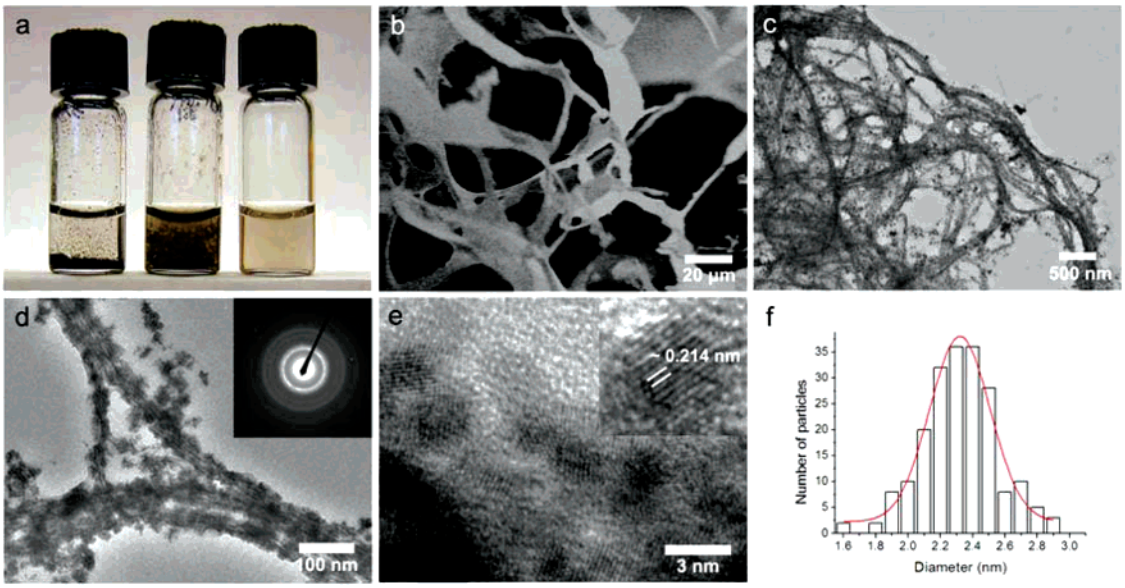


**Figure 2.** Synthesis of Co−Pt nanoparticles on fibrous phage template. (a) Solution after nucleation and growth of Co−Pt with wild-type (left), K17−$Co^{2+}$ (center), and no phage (right). (b) SEM image of the K17−$Co^{2+}$ sample after freeze-drying. (c) TEM image of the K17−$Co^{2+}$ sample. (d) TEM image showing bundled phage. Inset: SAED pattern of Co−Pt. (e) HRTEM of individual Co−Pt nanoparticles showing lattice fringes and a lattice spacing (inset). (f) Distribution of particle diameters from TEM images (average particle size = 2.3 nm).

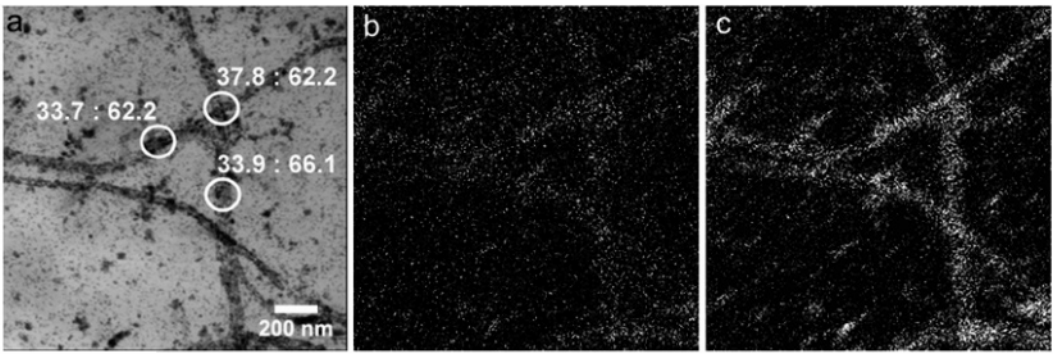


**Figure 3.** (a) STEM image of Co−Pt nanoparticles prepared on the fibrous phage bundle. Atomic ratios of Co and Pt on fibrous structure are shown. (b) Co and (c) Pt map showing distribution of Co and Pt.

diffraction (SAED) pattern shows the fundamental ring pattern of fcc CoPt.[23] A HRTEM image (Figure 2e) shows the lattice fringe of the nanoparticles, indicating their crystalline nature. The lattice spacing of the crystal is ~0.214 nm, which is in good agreement with the estimated values of 0.219 nm for [111] facet of fcc $Co_{0.35}Pt_{0.65}$ by Vegard's law.[24] The average particle size from the HRTEM is 2.3 nm (SD = 0.23 nm; Figure 2f).

M13 bacteriophage with partial peptide display on pVIII (type 8+8 phage) have previously been used as templates for synthesizing inorganic nanowires of semiconductors[25] and magnetic materials.[26,27] The random display of the selected peptide (7−12 amino acids) on pVIII in these reports produces the random variable in packing density of modified pVIII coat proteins along the phage and makes it difficult to always obtain identical structure. Unlike the type 8+8 systems, we obtained clearly defined inorganic placement on phage particles in the bundle structure. Individual phage with $Co_{0.35}Pt_{0.65}$ nanoparticles can be visualized with regular thickness of the inorganic layer.

STEM and EDS mapping were used for the chemical analysis of the $Co_{0.35}Pt_{0.65}$ hybrid material. Consistent atomic ratios of Co−Pt were observed (Figure 3a), showing regular composition along the fibrous phage template. Elemental mapping of Co and Pt (Figure 3b,c) on a fibrous phage template suggested that the nanocrystals on the template are alloys of Co and Pt.

The magnetic properties of the hybrid material were measured with DC SQUID. The zero-field-cooling (ZFC) and field-cooling (FC) magnetization (M) were monitored as a function of temperature (Figure 4a). The ZFC mode was carried out by cooling to 5 K in a zero field and then heating to 300 K in a 100 Oe field. Field cooling magnetization was achieved by cooling to 5 K and heating to 300 K in the presence of a 100 Oe field. The observed blocking temperature ($T_B$), which is the characteristic temperature with maximum ZFC magnetization, was 50 K. Typical superparamagnetic behavior of single domain nanoparticles was observed, showing divergence of the ZFC and FC curves below $T_B$ and coincidence of the curves over $T_B$. From the measured $T_B$ and average particle size, the estimated $K_{eff}$ is $2.7 \times 10^7$ ergs/cm$^3$ which is between the value for fcc $Co_{0.35}Pt_{0.65}$ film ($\sim 7 \times 10^6$ ergs/cm$^3$)[28] and the value for the ordered fct phase of CoPt ($\sim 5 \times 10^7$ ergs/cm$^3$). The high $K_{eff}$ can be explained by surface effects on magnetic anisotropy.[29] In addition, typical superparamagnetic behavior was observed from field dependent magnetization at 5 and 300 K (Figure 4b). Coercivity and remanence were zero above $T_B$, whereas an asymmetric hysteretic feature was observed below $T_B$ (coercivity $\approx$ 782 Oe), suggesting the presence of the exchange anisotropy, which is observed at the interface of ferromagnetic and antiferromagnetic materials.[30] Thus, it is possible that an antiferromagnetic oxide layer could be present.

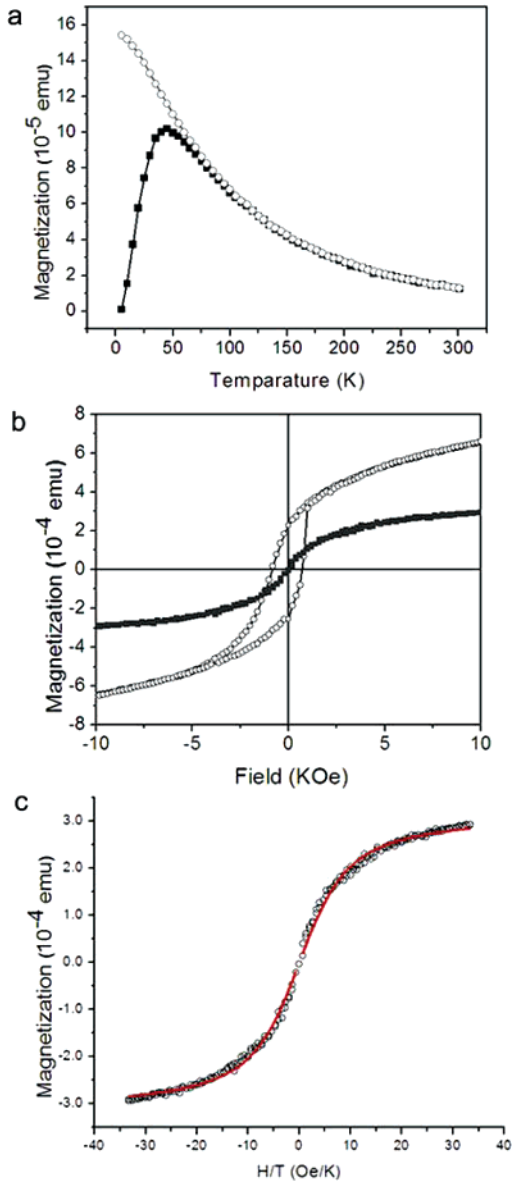


**Figure 4.** SQUID characterization of $Co_{0.35}Pt_{0.65}$ hybrid materials. (a) ZFC (solid rectangle) and FC (open circle) magnetization as a function of temperature. (b) Magnetization versus applied magnetic field at 5 K (solid rectangle) and 300 K (open circle). (c) Fit for the Langevin function at 300 K (red line).

We also believe that the interaction between the nanoparticles and the phage matrix can contribute to the asymmetric hysteresis behavior. The magnetization curve at 300 K was well fitted to the Langevin function (Figure 4c). The magnetic moment per Co−Pt particles was calculated to be 4008 $\mu_B$ (Bohr magneton).

## Conclusions

In this communication, we have described the selection of genetically modified type 8 phage particles having affinity to a metal ion and the metal-ion mediated bundle formation of these particles at low phage concentrations. The spongelike morphology of phage bundles was used as a template to nucleate Co−Pt nanoparticles which are both regularly located on the phage structure and show a narrow size distribution. The hybrid material showed typical superparamagnetic properties with high anisotropy. We believe that the introduced method can be used for other inorganic materials, such as metals and semiconductors. The further modification of the pVIII display library to include modified gene III and gene IX will allow for additional peptides to be displayed on the phage capsid to simultaneously organize multiple types of inorganic materials.

**Acknowledgment.** We acknowledge support from Army Research Office, Institute of Collaborative Biotechnologies, and the David and Lucile Packard Foundation.

**Supporting Information Available.** TEM images of Co−Pt particles without phage and with wild-type phage. This material is available free of charge via the Internet at http://pubs.acs.org.

## References and Notes

(1) Yan, H.; Park, S. H.; Finkelstein, G.; Reif, J. H.; LaBean, T. H. *Science* **2003**, *301*, 1882−1884.
(2) Vauthey, S.; Santoso, S.; Gong, H. Y.; Watson, N.; Zhang, S. G. *Proc. Natl. Acad. Sci. U.S.A.* **2002**, *99*, 5355−5360.
(3) Petka, W. A.; Harden, J. L.; McGrath, K. P.; Wirtz, D.; Tirrell, D. A. *Science* **1998**, *281*, 389−392.
(4) Weiner, S.; Traub, W.; Wagner, H. D. *J. Struct. Biol.* **1999**, *126*, 241−255.
(5) Weiner, S.; Wagner, H. D. *Annu. Rev. Mater. Sci.* **1998**, *28*, 271−298.
(6) Cha, J. N.; Shimizu, K.; Zhou, Y.; Christiansen, S. C.; Chmelka, B. F.; Stucky, G. D.; Morse, D. E. *Proc. Natl. Acad. Sci. U.S.A.* **1999**, *96*, 361−365.
(7) Shimizu, K.; Cha, J.; Stucky, G. D.; Morse, D. E. *Proc. Natl. Acad. Sci. U.S.A.* **1998**, *95*, 6234−6238.
(8) Hirano, S.; Nakahira, T.; Nakagawa, M.; Kim, S. K. *J. Biotechnol.* **1999**, *70*, 373−377.
(9) Falini, G.; Albeck, S.; Weiner, S.; Addadi, L. *Science* **1996**, *271*, 67−69.
(10) Shen, X. Y.; Belcher, A. M.; Hansma, P. K.; Stucky, G. D.; Morse, D. E. *J. Biol. Chem.* **1997**, *272*, 32472−32481.
(11) Whaley, S. R.; English, D. S.; Hu, E. L.; Barbara, P. F.; Belcher, A. M. *Nature* **2000**, *405*, 665−668.
(12) Brown, S. *Nat. Biotechnol.* **1997**, *15*, 269−272.
(13) Lee, S. W.; Mao, C. B.; Flynn, C. E.; Belcher, A. M. *Science* **2002**, *296*, 892−895.
(14) Naik, R. R.; Stringer, S. J.; Agarwal, G.; Jones, S. E.; Stone, M. O. *Nat. Mater.* **2002**, *1*, 169−172.
(15) Petrenko, V. A.; Smith, G. P.; Gong, X.; Quinn, T. *Protein Eng.* **1996**, *9*, 797−801.
(16) Lin, X. M.; Sorensen, C. M.; Klabunde, K. J.; Hajipanayis, G. C. *J. Mater. Res.* **1999**, *14*, 1542−1547.
(17) Kim, D. K.; Zhang, Y.; Voit, W.; Rao, K. V.; Muhammed, M. *J. Magn. Magn. Mater.* **2001**, *225*, 30−36.
(18) Kumar, D.; Pennycook, S. J.; Lupini, A.; Duscher, G.; Tiwari, A.; Narayan, J. *Appl. Phys. Lett.* **2002**, *81*, 4204−4206.
(19) Xing, G.; DeRose, V. J. *Curr. Opin. Chem. Biol.* **2001**, *5*, 196−200.
(20) Lombardi, A.; Summa, C. M.; Geremia, S.; Randaccio, L.; Pavone, V.; DeGrado, W. F. *Proc. Natl. Acad. Sci. U.S.A.* **2000**, *97*, 6298−6305.
(21) Muthukumar, M.; Ober, C. K.; Thomas, E. L. *Science* **1997**, *277*, 1225−1232.
(22) Lee, S. W.; Lee, S. K.; Belcher, A. M. *Adv. Mater.* **2003**, *15*, 689−692.
(23) Huang, Y. H.; Zhang, Y.; Hadjipanayis, G. C.; Simopoulos, A.; Weller, D. *IEEE T. Magn.* **2002**, *38*, 2604−2606.
(24) Petit, C.; Rusponi, S.; Brune, H. *J. Appl. Phys.* **2004**, *95*, 4251−4260.
(25) Mao, C. B.; Flynn, C. E.; Hayhurst, A.; Sweeney, R.; Qi, J. F.; Georgiou, G.; Iverson, B.; Belcher, A. M. *Proc. Natl. Acad. Sci. U.S.A.* **2003**, *100*, 6946−6951.
(26) Reiss, B. D.; Mao, C. B.; Solis, D. J.; Ryan, K. S.; Thomson, T.; Belcher, A. M. *Nano Lett.* **2004**, *4*, 1127−1132.
(27) Mao, C.; Solis, D. J.; Reiss, B. D.; Kottmann, S. T.; Sweeney, R. Y.; Hayhurst, A.; Georgiou, G.; Iverson, B.; Belcher, A. M. *Science* **2004**, *303*, 213-217.
(28) Shapiro, A. L.; Rooney, P. W.; Tran, M. Q.; Hellman, F.; Ring, K. M.; Kavanagh, K. L.; Rellinghaus, B.; Weller, D. *Phys. Rev. B* **1999**, *60*, 12826−12836.
(29) Hickey, B. J.; Howson, M. A.; Greig, D.; Wiser, N. *Phys. Rev. B* **1996**, *53*, 32−33.
(30) Mejia-Lopez, J.; Soto, P.; Altbir, D. *Phys. Rev. B* **2005**, *71*, 104422.

BM050691X